


Article

The Importance of Being Asymmetric for Geophysical Vortices

Georgi G. Sutyrin 

Graduate School of Oceanography, University of Rhode Island, Narragansett, RI 02882, USA; gsutyrin@uri.edu

Abstract: Several types of spatial symmetry in vortex structures within rotating stratified fluids are examined by looking at self-propagating configurations in the quasigeostrophic model. The role of symmetry breaking in the dynamics of geophysical waves, vortices and instabilities is highlighted. In particular, the energy exchange of the large-scale vertical shear with monopolar and dipolar vortices is analyzed. Various coupled vortex-wave structures are described in terms of wavy and evanescent modes. The Rossby wave radiation is shown to induce a zonal asymmetry, which is needed for the energy support and self-amplification of vortices in large-scale flow. The consequences for the evolution of the most long-lived vortices in the subtropical westward flows are discussed.

Keywords: baroclinic vortices; spatial symmetry; heat transport

1. Introduction

Symmetry plays a fundamental role in the understanding of physical processes and mathematical models. Generally, breaking symmetry and subsequent transitions can be related to internal instabilities as well as external forces. Rich flow patterns in rotating and stratified fluids stimulate the exploration of vortex dynamics and symmetries for a long time. Some of the results have been summarized in books and reviews, e.g., Khain and Sutyrin [1], McWilliams [2], Flierl [3], Korotaev [4], Carton [5] and Sokolovskii and Verron [6]. Here, we examine the role of rotational and mirror symmetries in the context of geophysical vortices such as monopoles and dipoles, which are abundant in atmospheric and oceanic flows (Chelton et al. [7] and Ni et al. [8]).

Baroclinic vortices (also called eddies) with nearly vertical axes dominate in the kinetic energy of mesoscale variability, transporting masses of water in their cores for thousands of kilometers (Dong et al. [9]). They often persist for many rotational periods, challenging parameterization schemes of mesoscale eddies in the global numerical models of climate variability (e.g., Thompson and Young [10], Gallet and Ferrari, [11], Ryzhov and Berloff, [12] and Sutyrin et al. [13]).

For several decades, it has remained puzzling how long-lived vortices survive in strongly variable environments with significant background gradients of potential vorticity (PV) supportive to the Rossby wave radiation. A number of zonally propagating nonlinear, non-radiating solutions to the equations of motion of rotating fluids were constructed at the beta plane without any background flow. The first examples of modon-like dipoles, introduced by Stern [14] and Larichev and Reznik [15], originated from a self-propelling classical Lamb–Chaplygin dipole (Lamb [16] and Meleshko and van Heijst [17]). Generally, quasigeostrophic (QG) modons avoid radiating Rossby waves by choosing the zonal drift of an active dipole for evanescent modes with a speed that is outside the range of wavy linear modes (see Kizner et al. [18]).

The dipolar component was found to be unnecessary for non-radiating zonally drifting monopolar anticyclones (Mikhailova and Shapiro [19], Petviashviliy [20] and Sutyrin [21]). This sparked a great interest in the dynamic differences between cyclones and anticyclones larger than the radius of deformation in more general intermediate geostrophic models (Nezlin and Sutyrin [22] and Sutyrin and Yushina [23]). The self-intensification of ed-



Citation: Sutyrin, G.G. The Importance of Being Asymmetric for Geophysical Vortices. *Symmetry* **2023**, *15*, 2204. <https://doi.org/10.3390/sym15122204>

Academic Editor: Rainer Hollerbach

Received: 12 November 2023

Revised: 7 December 2023

Accepted: 12 December 2023

Published: 15 December 2023



Copyright: © 2023 by the author. Licensee MDPI, Basel, Switzerland. This article is an open access article distributed under the terms and conditions of the Creative Commons Attribution (CC BY) license (<https://creativecommons.org/licenses/by/4.0/>).

dies in homogeneous environments owing to the non-adiabatic redistribution of angular momentum was described for both vortex polarities (Sutyrin [24]).

Satellite data on real oceanic vortices also indicate a significant meridional drift, which is particularly important for meridional heat transport [7,9]. Idealized models of radiating vortices in the ocean at rest demonstrated the relation of the meridional drift to the Rossby wave generation (Flierl [25], Korotaev [26] and Nycander [27]). The gradual decay of such nonlinear radiating vortices is slower than the decay of the linear Rossby wave packet. This is related to the Lagrangian invariance of PV inside the vortex core, with closed PV isolines supported by the processes of axisymmetrization in fast rotating vortices (Sutyrin [28] and Reznik and Kravtsov [29]).

In reality, eddies interact with large-scale currents, having an enormous reservoir of available potential energy (APE) in the main thermocline, storing roughly 1000 times more APE than the kinetic energy (KE) associated with its thermal-wind current shear (Gill et al. [30]). The majority of large-scale ocean currents have changing sign of background PV gradients affected by sloping isopycnals and mesoscale variability, which can be related to baroclinic instability (Vallis [31]). The spatial scales of linear baroclinic instability are in approximate agreement with observations, so that the eddy KE is believed to be supported by the mean APE in vertically sheared unstable flows (Ferrari and Wunsch [32]). Similar conclusions are also provided by eddy-resolving numerical models, where the barotropic and the first baroclinic modes dominate in the eddy field (Venaille et al. [33]). Therefore, two-layer models with bottom friction still play an important quantitative role in the numerical exploration of the typical scales and nonlinear saturation of eddies (e.g., Gallet and Ferrari [11], Radko et al. [34] and Sutyrin and Radko [35]).

The capacity of the vertical shear to support nonlinear steady radiating vortices was found recently for marginally stable zonal flows (Sutyrin et al. [36]). The baroclinic vortices were shown to be coupled with the lee Rossby waves, resulting in their meridional drift and heat flux, while their energy loss to the Rossby waves is compensated by the APE in the mean flow. Such meridional drift leads to eddy self-intensification, as confirmed numerically in baroclinically unstable flows with bottom friction (Sutyrin et al. [37]).

Here, we consider the symmetry properties of steady propagating states in the presence of vertical shear affecting the background PV gradient. We also show the importance of zonal asymmetry related to lee Rossby waves for effective meridional transport by long-lived eddies. This paper is organized as follows: the two-layer QG model is described in Section 2; the relations between different spatial symmetries are considered in Section 3; non-radiating as well as radiating steady propagating states are explored in Section 4; and the results, as well as how they can be interpreted from the perspective of previous studies and the working hypotheses, are discussed in Section 5, where several unresolved problems that deserve further investigation are mentioned.

2. Quasigeostrophic Model and Integral Invariants

We start with the commonly used two-layer model with the depths of the upper and lower layer (H_1, H_2). The basic flow is represented by laterally uniform zonal velocity (U_1, U_2) in local Cartesian coordinates, (X, Y), with positive X representing eastward and positive Y representing poleward on the beta plane (the Phillips model). The inviscid evolution of flow perturbations is described by the material conservation of the Lagrangian potential vorticity, $q_j + \beta_j y$ (Pedlosky [38]):

$$D_t(q_j + \beta_j y) = 0, \quad D_t \equiv \partial_t + (u_j + \bar{u}_j)\partial_x + v_j\partial_y \quad (1)$$

Here, we use nondimensional variables introducing the velocity scale, U , and the spatial scale, L . In the QG approximation, the perturbation velocity, (u_j, v_j) , and the potential vorticity, q_j , are expressed by the geopotential, p_j :

$$u_j = -\partial_y p_j, \quad v_j = \partial_x p_j, \quad q_j = \left(\partial_x^2 + \partial_y^2\right)p_j + \frac{(-1)^j}{h_j}(p_1 - p_2), \quad (2)$$

$$\beta_j = \beta - \frac{(-1)^j}{h_j}(\bar{u}_1 - \bar{u}_2) \quad (3)$$

where $h_j = g'H_j/f_0^2L^2$, g' is the reduced gravity and f_0 is the Coriolis parameter.

$\beta = \beta_0L^2/U$, β_0 is the gradient of the Coriolis parameter and $\bar{u}_j = U_j/U$.

In order to understand the dynamics of geophysical vortices and their interaction with Rossby waves, it is important to consider the integral invariants. The first inviscid invariant is the pseudomomentum, $M = M_1 + M_2$, consisting of quadratic integrals:

$$M_j = -\frac{1}{2} \int h_j \frac{q_j^2}{\beta_j} dx dy, \quad j = 1, 2. \quad (4)$$

This is obtained by multiplying the equations in Equation (1) for each layer by $\frac{h_j q_j}{\beta_j}$, adding the results and integrating over the xy -plane (see [36]). It follows from Equation (4) that if β_1 and β_2 are both positive, M is negative definite; therefore, perturbations cannot grow, and such flow is stable. On the other hand, if $\beta_1 < 0$ or $\beta_2 < 0$, such flow is baroclinically unstable (Phillips [39]). If $M = 0$ initially, it is conserved, and a growing mode involves momentum transfer between the layers.

Another inviscid integral invariant, the pseudoenergy E , is obtained by multiplying the equations in Equation (1) for each layer by $h_j p_j$, adding the results and integrating them over the xy -plane:

$$E = E_1 + E_2 + E_p + \bar{u}_1 M_1 + \bar{u}_2 M_2 \quad (5)$$

Here, the perturbation kinetic energy in the two layers and the perturbation available potential energy are as follows:

$$E_j = \frac{h_j}{2} \int (\nabla p_j)^2 dx dy, \quad E_p = \frac{1}{2} \int (p_1 - p_2)^2 dx dy, \quad (6)$$

The last two terms in Equation (5) reflect an energy exchange between the perturbation and the background state. The rate of change in this interaction energy is defined by the meridional PV flux (PVF) in the upper layer:

$$PVF \equiv h_1 \int q_1 v_1 dx dy = \frac{dM_1}{dt} = -\frac{h_1 + h_2}{h_1 h_2} F_h \quad (7)$$

which is proportional to the heat flux

$$F_h = \int (p_1 - p_2) \frac{\partial}{\partial x} (h_1 p_1 + h_2 p_2) dx dy, \quad (8)$$

according to the Taylor–Bretherton relationship.

Considering that E is the inviscid invariant, the energy of perturbations can grow

$$\frac{d}{dt} (E_1 + E_2 + E_p) = (\bar{u}_2 - \bar{u}_1) \frac{dM_1}{dt} \quad (9)$$

when either $\beta_1 < 0$ in the westward background (WB) flow ($\bar{u}_1 < \bar{u}_2$) or $\beta_2 < 0$ in the eastward background (EB) flow ($\bar{u}_1 > \bar{u}_2$), indicating that such background flows are unstable, in agreement with Equation (4). Thus, the energy can be released from the background state by equatorward heat flux in the WB flow and poleward heat flux in the EB flow.

3. Spatial Symmetries

Here, we consider the circular, meridional and zonal symmetry properties of geophysical vortices, starting with different types of meridional symmetry relative to the zonal axis. According to Reznik [40], the flow can be uniquely decomposed into two components,

$$p_j(x, y, t) = p_j^A(x, y, t) + p_j^S(x, y, t) \quad (10)$$

$$p_j^A = \frac{p_j(x, y, t) + p_j(x, -y, t)}{2}, \quad p_j^S = \frac{p_j(x, y, t) - p_j(x, -y, t)}{2} \quad (11)$$

representing even and odd parts of the streamfunction, and producing antisymmetric u_j^A and symmetric u_j^S zonal velocity, respectively. Here, the notations for the A- and S-components follow those described by Brion et al. [41] and Davies et al. [42,43], which are opposite relative to those described by Reznik [40]. For example, the A-component represents a circular symmetric vortex (Figure 1a) and a meridionally propagating A-dipole (Figure 1b), while a zonally propagating S-dipole is described by the S-component (Figure 1c).

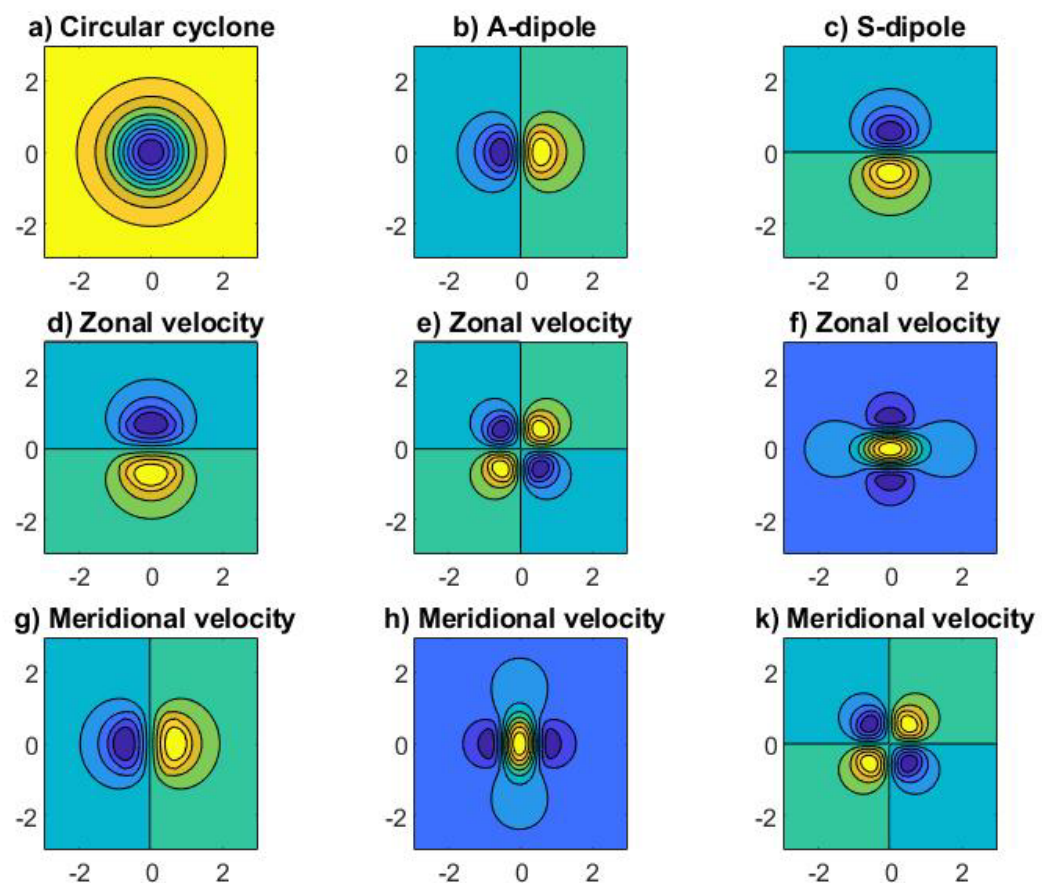


Figure 1. The geopotential, zonal velocity and meridional velocity in a circular cyclone (a,d,g); in a meridional A-dipole (b,e,h); and in a zonal S-dipole (c,f,k).

Following the procedure suggested by Reznik [40], from Equations (1)–(3), we obtain the following for each component:

$$D_t^S q_j^A + \beta_j \partial_x p_j^A = -(u_j^A \partial_x + v_j^A \partial_y) q_j^S \equiv J(q_j^S, p_j^A) \quad (12)$$

$$D_t^S q_j^S + \beta_j \partial_x p_j^S = -(u_j^A \partial_x + v_j^A \partial_y) q_j^A \equiv J(q_j^A, p_j^A) \quad (13)$$

$$D_t^S \equiv \partial_t + (u_j^S + \bar{u}_j)\partial_x + v_j^S\partial_y \quad (14)$$

For a single layer without any basic flow, it was noted by Reznik [40] that the S-component looks sufficient to describe the evolution when the A-component is zero initially, as in various types of modon solutions, e.g., Larichev–Reznik dipole (LRD) [15]. However, an instability of the trajectory of westward propagating LRD, described by Nycander and Isichenko [44], is associated with spontaneous tilting resulting in the appearance of the A-component, a so-called T-mode (Figure 1 in [43]). Another type of spontaneous symmetry breaking was found in [42] for the eastward propagating LRD due to the development of a growing unstable A-mode (Figure 2 in [43]), confirming the long-standing difficulty of rigorously proving its stability (Nycander [45]).

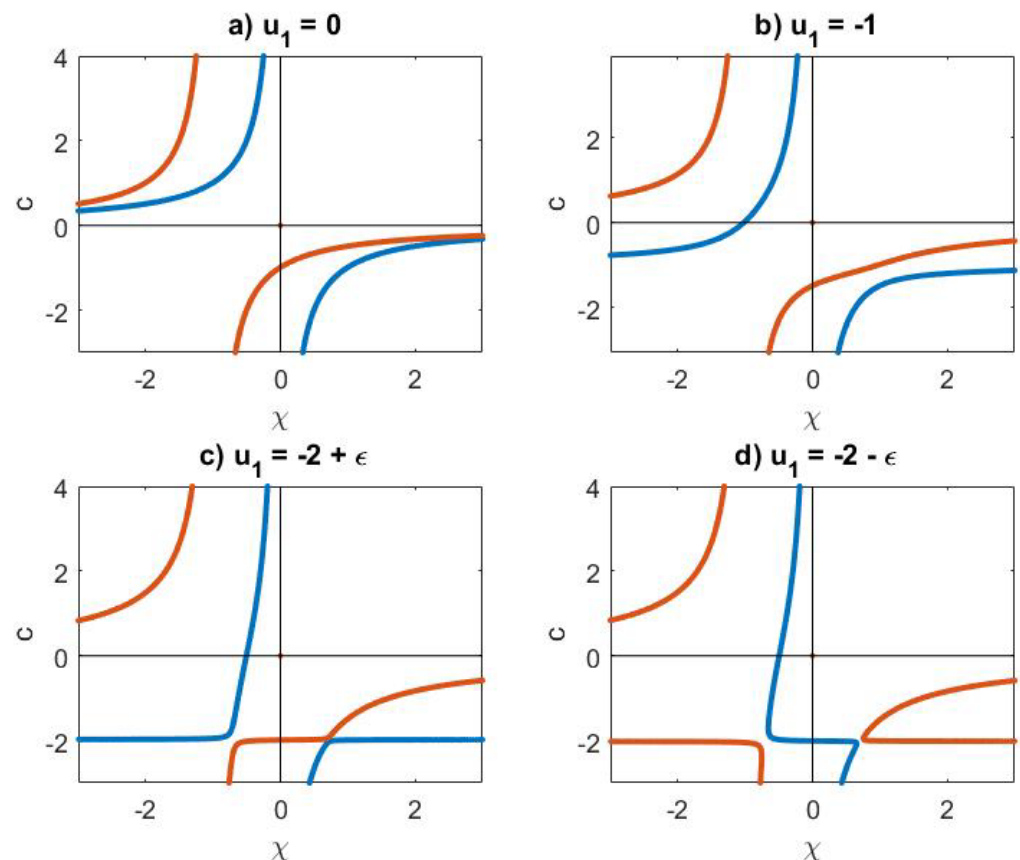


Figure 2. The branches of evanescent and wavy modes for different values of the vertical shear in the WB flow: BC (red) and BEQT (blue) modes according to (23) (a); the effects of the vertical shear on the branches originating from BC and BT modes (b); the reconnection of branches near the marginal stability (c); and weakly unstable flow (d).

On the other hand, as seen in Equation (13), a non-zero A-component generates an S-component even if it was zero initially, unless $J(p_j^A, q_j^A)$ remains zero, as in the circular symmetric monopolar vortex. However, breaking the circular symmetry of monopolar vortices owing to barotropic and/or baroclinic instability results in nonzero $J(p_j^A, q_j^A)$, even without the beta effect (e.g., Sutyrin [46] and references therein).

To emphasize the importance of zonal asymmetry at the beta plane, we suggest the further decomposition of A- and S-components

$$p_j^{A,S}(x, y, t) = p_{j,E}^{A,S}(x, y, t) + p_{j,O}^{A,S}(x, y, t) \quad (15)$$

$$p_{j,E}^{A,S} = \frac{p_j^{A,S}(x,y,t) + p_j^{A,S}(-x,y,t)}{2}, \quad p_{j,O}^{A,S} = \frac{p_j^{A,S}(x,y,t) - p_j^{A,S}(-x,y,t)}{2} \quad (16)$$

representing zonally even and odd parts of A- and S-components, producing zonally antisymmetric $v_{j,E}^{A,S}$ and symmetric $v_{j,O}^{A,S}$ meridional velocity, respectively. Even without a vertical shear, the circular symmetric vortex represented by $p_{j,E}^A$ (Figure 1a) first generates a dipole propagating meridionally described by $p_{j,O}^A$ (Figure 1b), which results in the development of a dipole propagating zonally ($p_{j,E}^S$, Figure 1c) (Sutyrin [47,48]). Note that the vertical shear strongly affects the vortex evolution (Vandermeirsh et al. [49]).

In the presence of vertical shear, the energy exchange Equation (9) is proportional to the following:

$$\begin{aligned} PVF &\equiv h_1 \int (q_1^A + q_1^S)(v_1^A + v_1^S) dx dy = h_1 \int (q_1^A v_1^A + q_1^S v_1^S) dx dy = \\ &= h_1 \int (q_{1,E}^A v_{1,O}^A + q_{1,O}^A v_{1,E}^A + q_{1,E}^S v_{1,O}^S + q_{1,O}^S v_{1,E}^S) dx dy \end{aligned} \quad (17)$$

Thus, while A- and S-components contribute to PVF separately, both zonally symmetric and antisymmetric parts are needed for the energy exchange with the large-scale flow. Further, we consider the symmetry properties of steady propagating vortex structures.

4. Steady Propagating Structures

4.1. Evanescent and Wavy Modes

For a steady state in translating coordinates $(x - ct, y)$, Equation (1) becomes the following:

$$J(\psi_j, q_j + \beta_j y) = 0 \quad (18)$$

Generally, this means that the potential vorticity in each layer $q_j + \beta_j y$ follows streamlines of $\psi_j = p_j + (-\bar{u}_j + c)y$ in moving coordinates. The functional dependence $q_j + \beta_j y = F_j(\psi_j)$ is uniquely defined only in the exterior region with open streamlines:

$$(c - \bar{u}_j)q_j = \beta_j p_j \quad (19)$$

In the exterior region, the solution for two layers is described by decoupled modes $\phi_k = p_1 + \alpha_k p_2$, where α_k are roots of the quadratic equation:

$$\frac{\alpha^2}{h_2} - \frac{\alpha}{h_1} - \frac{\alpha\beta_1}{c - \bar{u}_1} = \frac{1}{h_1} - \frac{\alpha}{h_2} - \frac{\alpha\beta_2}{c - \bar{u}_2} \quad (20)$$

$$\alpha = d \mp \sqrt{d^2 + \frac{h_2}{h_1}}, \quad d = \frac{1}{2} \left(\frac{h_2}{h_1} - 1 + \frac{h_2\beta_1}{c - \bar{u}_1} - \frac{h_2\beta_2}{c - \bar{u}_2} \right) \quad (21)$$

Thus, there are always two real values of χ_k for the decoupled system:

$$\left(\partial_x^2 + \partial_y^2 + \chi_k \right) \phi_k = 0 \quad \chi_k = \frac{\alpha_k}{h_2} - \frac{1}{h_1} - \frac{\beta_1}{c - \bar{u}_1} \quad (22)$$

where the type of the solution depends on the sign of χ_k : wavy mode (if $\chi_k > 0$) and evanescent mode (if $\chi_k < 0$).

Without basic flow over a flat bottom, $\alpha_1 = -1$ and $\alpha_2 = \frac{h_2}{h_1}$ correspond to baroclinic (BC) and barotropic (BT) vertical modes:

$$\chi_1 = \chi_{BC} = -\frac{1}{h_1} - \frac{1}{h_2} - \frac{\beta}{c}, \quad \chi_2 = \chi_{BT} = -\frac{\beta}{c} \quad (23)$$

The zonal phase speed of planar Rossby waves for $\chi_k = l^2 + m^2 > 0$, assuming $\phi_k \sim \exp(ilx + imy)$, is well known to be negative

$$-\frac{1}{\gamma^2} < \frac{c_{BC}}{\beta} = -\frac{1}{l^2 + m^2 + \gamma^2} < 0 < \frac{c_{BT}}{\beta} = -\frac{1}{l^2 + m^2} < 0 \quad (24)$$

where $\gamma^2 = \frac{1}{h_1} + \frac{1}{h_2}$ denotes the reciprocal squared radius of deformation. Examples of BC and BT branches at the plane (χ, c) are shown in Figure 2a, where $h_1 = h_2 = 2$ is chosen, so that $\gamma = 1$. We see that both branches of the eastward propagating BC and BT modes are evanescent (if $c > 0$, $\chi_1 < 0$ and $\chi_2 < 0$, in the upper part of Figure 2a).

4.2. Nonradiating Vortex Structures

Generally, in the polar coordinates (r, θ) , the far field of localized states with both evanescent modes (when $\chi_1 < 0$ and $\chi_2 < 0$), the solution to Equation (22) is described by modified Bessel functions:

$$\phi_k = \sum_0^{\infty} K_n(r\sqrt{-\chi_k})(a_n \cos n\theta + b_n \sin n\theta) \quad (25)$$

Without the vertical shear over the flat bottom, a fast propagating westward BC evanescent mode (when $\frac{c}{\beta} < -\frac{1}{\gamma^2}$) coexists with the BT wavy mode (when $\chi_1 < 0$ and $\chi_2 > 0$, see the lower part of Figure 2a). In this case, the far field of radiating states may include the weakly decaying wavy mode described by Bessel functions, J_n :

$$\phi_2 = \sum_0^{\infty} J_n(r\sqrt{\chi_2})(a_n \cos n\theta + b_n \sin n\theta) \quad (26)$$

In the presence of the basic flow, it is also possible to construct localized solutions for the zonal propagation speed, satisfying both $\chi_1 < 0$ and $\chi_2 < 0$ (regular modons), or when the wavy mode is zero in the exterior, even if $\chi_1 < 0$ and $\chi_2 > 0$ (anomalous modons), according to Flierl et al. [50]. Denoting the position $(x_c(t), y_c(t))$ of the centre of the structure, the flow field is described by the following streamfunction:

$$\psi_j = p_j + (-\bar{u}_j + c)rsin(\theta), \quad \dot{x}_c = c \dot{y}_c = 0 \quad (27)$$

In the case of steady propagation, isolines of ψ_j describe the particles' trajectories both outside and inside the separatrix, where

$$q_j + \beta_j r \sin \theta = F_j(\psi_j) \quad (28)$$

Commonly, the linear functions $F_j(\psi_j) = -\kappa_j^2 \psi_j$ are used inside a circular separatrix where $r < a$ either in one or both layers. The matching conditions are applied at $r = a$ to relate κ_j^2 with the drift speed c . Therefore, the simplest possible solutions include only a dipolar component, $p_{j,E}^S$, proportional to $rsin\theta$, which is zonally symmetric, so that PVF = 0 in Equation (17). The general analysis of possible localized states can be performed in the same way as for the beta plane with topography but without large-scale flow (Kizner [18]). A circular symmetric rider, $p_{j,E}^A$, can be added, however, resulting in PVF = 0 in Equation (17) for non-radiating solutions due to zonal mirror symmetry relative to the y-axis in moving coordinates. Thus, there is no energy exchange between non-radiating structures and the large-scale flow.

4.3. Radiating Vortex Structures

Without shear, the radiating states are nonstationary and decay gradually, losing their energy to the Rossby wave radiation; westward propagating dipoles shrink (Haines Flierl [51], Crowe and Johnson [52]), while the vortices with dominant monopolar parts

drift both westward and meridionally (cyclones—poleward, anticyclones—equatorward) toward their latitude of rest inversely proportional to β (Korotaev [4] and Sutyryn [48]). Generally, the radiating states include a zonal dipole, $p_{j,E}^S$, in the interior together with the corresponding wavy mode in the exterior (Nycander [27]).

The vertical shear modifies the evanescent and wavy modes (see Figure 2), and provides an opportunity for monopolar vortices to drift both zonally and meridionally without decay, while radiating Rossby waves are supported by the energy flux Equation (9) with nonzero PVF. In particular, this was demonstrated for marginally stable zonal flows when either $|\beta_1| = 0$ or $|\beta_2| = 0$ in [36]. In the vicinity of marginally stable WB flow, choosing $c \approx \bar{u}_1$ allows us to satisfy Equation (19) for an arbitrary PV anomaly in the upper layer, while the evanescent and wavy modes correspond to the crossing of branches illustrated in Figure 2c,d:

$$-\chi_1 = \chi_2 = \gamma / \sqrt{h_1} \equiv \varkappa^2$$

Then, a given circular PV anomaly in the upper layer, $q_{1,E}^A(r)$, induces both the localized evanescent mode, which is also circular and zonally symmetric,

$$\phi_1 = K_0(\varkappa r) \int_0^r r' dr' I_0(\varkappa r') q_{1,E}^A(r') + I_0(\varkappa r) \int_r^\infty r' dr' K_0(\varkappa r') q_{1,E}^A(r'), \quad (29)$$

and the wavy mode, which includes zonally symmetric as well as antisymmetric parts owing to the inviscid solution being restricted by the condition that the far field vanishes to the west, resulting in lee Rossby waves to the east:

$$\phi_2 = \frac{\pi}{2} Y_0(\varkappa r) \int_0^r r' dr' J_0(\varkappa r') q_{1,E}^A(r') + \frac{\pi}{2} J_0(\varkappa r) \int_r^\infty r' dr' Y_0(\varkappa r') q_{1,E}^A(r') + W, \quad (30)$$

$$W = 2Z \sum_{n=1}^{\infty} \frac{\cos(2n-1)\theta}{2n-1} J_{2n-1}(\varkappa r), \quad Z = \int_0^\infty r' dr' J_0(\varkappa r') q_{1,E}^A(r') \quad (31)$$

The flow in each layer is a combination of the evanescent and wavy modes given by

$$p_1 = \frac{(1+\delta)\phi_1 + (1-\delta)\phi_2}{2h_1} \quad \text{and} \quad p_2 = \delta \frac{\phi_2 - \phi_1}{2h_2}, \quad \delta = \frac{1}{\varkappa^2 h_1} \quad (32)$$

This results in nonzero PVF in Equation (17)

$$PVF = h_1 \int q_{1,E}^A v_{1,O}^A dx dy \quad (33)$$

owing to the zonally symmetric component of meridional velocity $v_{1,O}^A \sim (1-\delta)\partial_x W$, where W is related to the lee Rossby waves in Equation (31). Figure 3 shows an example of such solution for

$$q_{1,E}^A(r) = J_0(r), \quad r < r_0 \quad \text{and} \quad q_{1,E}^A(r) = 0, \quad r > r_0 \quad (34)$$

where $h_1 = h_2 = 2$ is chosen to scale and $r_0 \approx 2.4$ is the first root of J_0 . In Figure 3d, one can see that the central part of $p_{1,O}^A$ is dominated by the A-dipole, similar to the one in Figure 1b.

Thus, we conclude that the zonal asymmetry related to the lee Rossby waves associated with the monopolar vortex is a major necessary component of long-lived eddies supported by the APE in the large-scale shear. Moreover, the meridional drift induced by the lee Rossby waves provides the self-amplification of the vortex in unstable flows ($\beta_1 < 0$) [37].

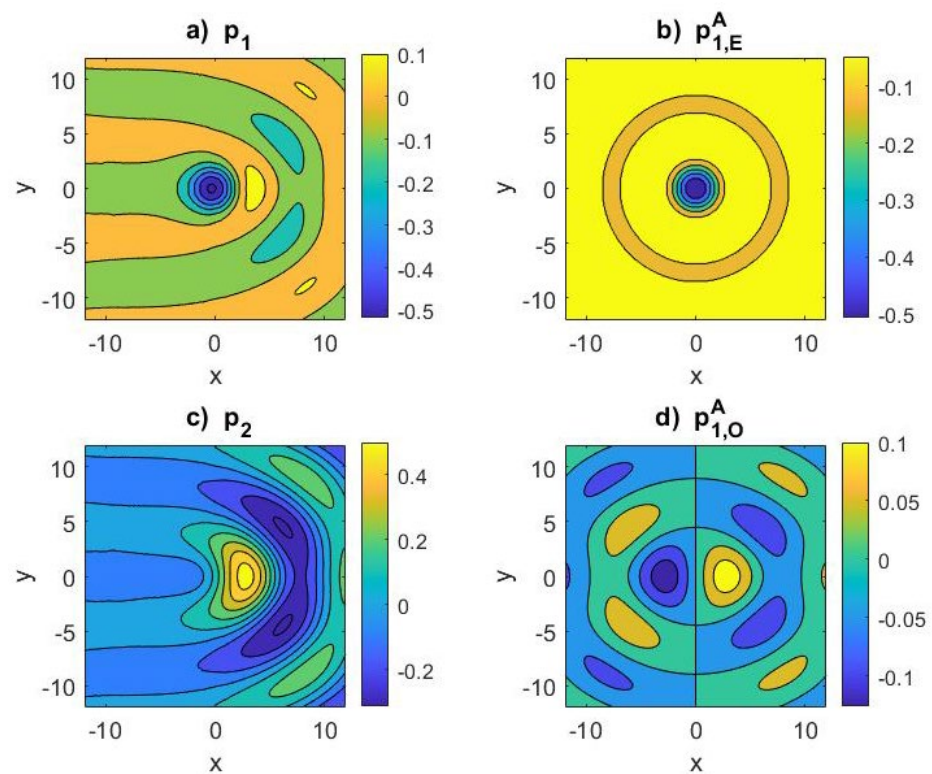


Figure 3. The geopotential Equation (32) in the upper (a) and lower (c) layers; zonally even (b) and odd (d) parts of the geopotential in the upper layer plotted in (a).

5. Discussion

We considered several types of spatial symmetry in self-propagating vortex configurations, focusing on their energy exchange with the large-scale vertical shear. The major focus is on the zonal asymmetry related to the basic west–east asymmetry of the system on the beta plane. The Rossby wave radiation is shown to be necessary to provide nonzero heat flux consistent with numerical simulations of baroclinic turbulence (e.g., Thomson and Young [10]). A general way to construct coupled vortex–wave structures is described in terms of wavy and evanescent modes. Non-radiating vortex structures are shown to have zero heat flux, owing to their zonal symmetry.

The ability of the vertical shear to support steady radiating monopolar vortices can be generalized to include a zonal dipolar component in the vicinity of marginally stable zonal flows. The theory shows that the major contribution to nonzero heat flux is provided by a combination of a circular symmetric PV anomaly and a zonally antisymmetric part of the lee Rossby waves; an additional zonal dipolar component is not essential. This analysis provides a physical interpretation of the self-amplifying hetons (SAH) that emerge spontaneously in numerical simulations [37].

The theory of steady radiating monopolar vortices is consistent with observations of the most long-lived vortices in the subtropical westward flows (Chen et al. [53]). The westward flows are characterized by sloping isopycnals that reduce the background PVG in the upper layer, which is only weakly affected by bottom friction. In contrast, the sloping isopycnals in the eastward flows reduce PVG in the lower layer, where bottom friction dominates in controlling the longevity of baroclinic vortices [35].

In the broad context, the further exploration of coupled vortex–wave structures and their symmetry properties should reveal basic elements on the way to building more adequate closure schemes of the heat transport in baroclinic turbulence. Future research directions may include inhomogeneous background flows, realistic stratification, cyclone–anticyclone asymmetry, inertia–gravity waves, bottom topography, continental boundaries, atmospheric forcing, etc.

Funding: This research was funded by the US National Science Foundation, grant number NSF-OCE-1828843.

Data Availability Statement: Data are contained within the article.

Acknowledgments: The author thanks Irina Kuzina for stimulating discussions and three anonymous reviews for their valuable comments.

Conflicts of Interest: The author declares no conflict of interest.

References

1. Khain, A.P.; Sutyryn, G.G. *Tropical Cyclones and Their Interaction with the Ocean 1983*; Gidrometeoizdat: Saint Petersburg, Russia, 1983; 272p. (In Russian)
2. McWilliams, J.C. Submesoscale, coherent vortices in the ocean. *Rev. Geophys.* **1985**, *23*, 165–182. [[CrossRef](#)]
3. Flierl, G.R. Isolated eddy models in geophysics. *Annu. Rev. Fluid Mech.* **1987**, *19*, 493–530. [[CrossRef](#)]
4. Korotaev, G.K. *Theoretical Modelling of Synoptic Variability of the Ocean*; Naukova Dumka: Kiev, Ukraine, 1988; 160p. (In Russian)
5. Carton, X. Hydrodynamical Modeling of Oceanic Vortices. *Surv. Geophys.* **2001**, *22*, 179–263. [[CrossRef](#)]
6. Sokolovskii, M.A.; Verron, J. *Dynamics of Vortex Structures in a Stratified Rotating Fluid*; Book Series: Atmospheric and Oceanographic Sciences Library; Springer: New York, NY, USA, 2014; Volume 47, 382p. [[CrossRef](#)]
7. Chelton, D.B.; Schlax, M.G.; Samelson, R.M. Global observations of nonlinear mesoscale eddies. *Prog. Oceanogr.* **2011**, *91*, 167–216. [[CrossRef](#)]
8. Ni, Q.; Zhai, X.; Wang, G.; Hughes, C.W. Widespread Mesoscale Dipoles in the Global Ocean. *J. Geophys. Res. Oceans* **2020**, *125*, e2020JC016479. [[CrossRef](#)]
9. Dong, C.; McWilliams, J.C.; Liu, Y.; Chen, D. Global heat and salt transports by eddy movement. *Nat. Commun.* **2014**, *5*, 3294. [[CrossRef](#)]
10. Thompson, A.F.; Young, W.R. Scaling Baroclinic Eddy Fluxes: Vortices and Energy Balance. *J. Phys. Oceanogr.* **2006**, *36*, 720–738. [[CrossRef](#)]
11. Gallet, B.; Ferrari, R. A Quantitative Scaling Theory for Meridional Heat Transport in Planetary Atmospheres and Oceans. *AGU Adv.* **2021**, *2*, e2020AV000362. [[CrossRef](#)]
12. Ryzhov, E.; Berloff, P. On transport tensor of dynamically unresolved oceanic mesoscale eddies. *J. Fluid Mech.* **2022**, *939*, A7. [[CrossRef](#)]
13. Sutyryn, G.G.; Radko, T.; McWilliams, J.C. Contrasting eddy-driven transport in baroclinically unstable eastward currents and subtropical return flows. *Phys. Fluids* **2022**, *34*, 126605. [[CrossRef](#)]
14. Stern, M.E. Minimal properties of planetary eddies. *J. Mar. Res.* **1975**, *33*, 1–13.
15. Larichev, V.D.; Reznik, G.M. On two-dimensional solitary Rossby waves. *Dokl. Akad. Nauk.* **1976**, *231*, 1077–1079.
16. Lamb, H. *Hydrodynamics*, 2nd ed.; Cambridge University Press: Cambridge, UK, 1895.
17. Meleshko, V.; van Heijst, G. On Chaplygin’s investigations of two-dimensional vortex structures in an inviscid fluid. *J. Fluid Mech.* **1994**, *272*, 157–182. [[CrossRef](#)]
18. Kizner, Z.; Berson, D.; Reznik, G.; Sutyryn, G. The Theory of the Beta-Plane Baroclinic Topographic Modons. *Geophys. Astrophys. Fluid Dyn.* **2003**, *97*, 175–211. [[CrossRef](#)]
19. Mikhailova, E.I.; Shapiro, N.B. Two-dimensional model of synoptic disturbances evolution in the ocean. *Izv. Acad. Sci. USSR Phys. Atmos. Okeana* **1980**, *16*, 823.
20. Petviashvili, V.I. The Jovian Red Spot and drift soliton in plasma. *JETP Lett.* **1980**, *32*, 632.
21. Sutyryn, G.G. Theory of solitary anticyclones in a rotating liquid. *Dokl. Akad. Nauk SSSR Earth Sci.* **1985**, *280*, 38.
22. Nezlin, M.V.; Sutyryn, G.G. Problems of simulation of large, long-lived vortices in the atmospheres of the giant planets (Jupiter, Saturn, Neptune). *Surv. Geophys.* **1994**, *15*, 63–99. [[CrossRef](#)]
23. Sutyryn, G.G.; Yushina, I.G. Numerical modelling of the formation, evolution, interaction and decay of isolated vortices. In *Mesoscale/Synoptic Coherent Structures in Geophysical, Turbulence*; Nihoul, J.C.J., Jamart, B.M., Eds.; Elsevier: Amsterdam, The Netherlands, 1989; Volume 50, pp. 721–736. [[CrossRef](#)]
24. Sutyryn, G. How baroclinic vortices intensify resulting from erosion of their cores and/or changing environment. *Ocean. Model.* **2020**, *156*, 101711. [[CrossRef](#)]
25. Flierl, G.R. Rossby Wave Radiation from a Strongly Nonlinear Warm Eddy. *J. Phys. Oceanogr.* **1984**, *14*, 47–58. [[CrossRef](#)]
26. Korotaev, G. Radiating Vortices in Geophysical Fluid Dynamics. *Surv. Geophys.* **1997**, *18*, 567–618. [[CrossRef](#)]
27. Nycander, J. Drift Velocity of Radiating Quasigeostrophic Vortices. *J. Phys. Oceanogr.* **2001**, *31*, 2178–2185. [[CrossRef](#)]
28. Sutyryn, G.G. The beta-effect and the evolution of a localized vortex. *Sov. Phys. Dokl.* **1987**, *32*, 791–793.
29. Kravtsov, S.; Reznik, G. Numerical solutions of the singular vortex problem. *Phys. Fluids* **2019**, *31*, 066602. [[CrossRef](#)]
30. Gill, A.; Green, J.; Simmons, A. Energy partition in the large-scale ocean circulation and the production of mid-ocean eddies. *Deep. Sea Res. Oceanogr. Abstr.* **1974**, *21*, 499–528. [[CrossRef](#)]
31. Vallis, G.K. *Atmospheric and Oceanic Fluid Dynamics*; Cambridge University Press: Cambridge, UK, 2017.
32. Ferrari, R.; Wunsch, C. Ocean Circulation Kinetic Energy: Reservoirs, Sources, and Sinks. *Annu. Rev. Fluid Mech.* **2009**, *41*, 253–282. [[CrossRef](#)]
33. Venaille, A.; Vallis, G.K.; Smith, K.S. Baroclinic Turbulence in the Ocean: Analysis with Primitive Equation and Quasigeostrophic Simulations. *J. Phys. Oceanogr.* **2011**, *41*, 1605–1623. [[CrossRef](#)]
34. Radko, T.; de Carvalho, D.P.; Flanagan, J. Nonlinear Equilibration of Baroclinic Instability: The Growth Rate Balance Model. *J. Phys. Oceanogr.* **2014**, *44*, 1919–1940. [[CrossRef](#)]

35. Sutyrin, G.G.; Radko, T. Why the most long-lived eddies are found in the subtropical ocean westward flows. *Ocean. Model.* **2021**, *161*, 101782. [[CrossRef](#)]
36. Sutyrin, G.G.; Radko, T.; Nycander, J. Steady radiating baroclinic vortices in vertically sheared flows. *Phys. Fluids* **2021**, *33*, 031705. [[CrossRef](#)]
37. Sutyrin, G.; Radko, T.; McWilliams, J.C. Self-amplifying hetons in vertically sheared geostrophic turbulence. *Phys. Fluids* **2021**, *33*, 101705. [[CrossRef](#)]
38. Pedlosky, J. *Geophysical Fluid Dynamics*; Springer: Berlin/Heidelberg, Germany, 1987; Volume 710.
39. Phillips, N.A. Energy transformations and meridional circulations associated with simple baroclinic waves in a two level, quasi-geostrophic model. *Tellus* **1954**, *6*, 273–286. [[CrossRef](#)]
40. Reznik, G.M. On the structure and dynamics of a two-dimensional Rossby soliton. *Acad. Sci. USSR Oceanol.* **1987**, *27*, 536–539.
41. Brion, V.; Sipp, D.; Jacquin, L. Linear dynamics of the Lamb-Chaplygin dipole in the two-dimensional limit. *Phys. Fluids* **2014**, *26*, 064103. [[CrossRef](#)]
42. Davies, J.; Sutyrin, G.G.; Berloff, P. On the spontaneous symmetry breaking of eastward propagating dipoles. *Phys. Fluids* **2023**, *35*, 041707. [[CrossRef](#)]
43. Davies, J.; Sutyrin, G.G.; Crowe, M.N.; Berloff, P.S. Deformation and destruction of north-eastward drifting dipoles. *Phys. Fluids* **2023**, *35*, 0171909. [[CrossRef](#)]
44. Nycander, J.; Isichenko, M.B. Motion of dipole vortices in a weakly inhomogeneous medium and related convective transport. *Phys. Fluids B Plasma Phys.* **1990**, *2*, 2042–2047. [[CrossRef](#)]
45. Nycander, J. Refutation of stability proofs for dipole vortices. *Phys. Fluids A Fluid Dyn.* **1992**, *4*, 467–476. [[CrossRef](#)]
46. Sutyrin, G. Why compensated cold-core rings look stable. *Geophys. Res. Lett.* **2015**, *42*, 5395–5402. [[CrossRef](#)]
47. Sutyrin, G.G.; Flierl, G.R. Intense Vortex Motion on the Beta Plane: Development of the Beta Gyres. *J. Atmos. Sci.* **1994**, *51*, 773–790. [[CrossRef](#)]
48. Sutyrin, G.G.; Hesthaven, J.S.; Lynov, J.P.; Rasmussen, J.J. Dynamical properties of vortical structures on the beta-plane. *J. Fluid Mech.* **1994**, *268*, 103–131. [[CrossRef](#)]
49. Vandermeirsh, F.; Morel, Y.; Sutyrin, G. Resistance of a Coherent Vortex to a Vertical Shear. *J. Phys. Oceanogr.* **2002**, *32*, 3089–3100. [[CrossRef](#)]
50. Flierl, G.; Larichev, V.; McWilliams, J.; Reznik, G. The dynamics of baroclinic and barotropic solitary eddies. *Dyn. Atmos. Ocean.* **1980**, *5*, 1–41. [[CrossRef](#)]
51. Flierl, G.R.; Haines, K. The decay of modons due to Rossby wave radiation. *Phys. Fluids* **1994**, *6*, 3487–3497. [[CrossRef](#)]
52. Crowe, M.N.; Johnson, E.R. The evolution of surface quasi-geostrophic modons on sloping topography. *J. Fluid Mech.* **2023**, *970*, A10. [[CrossRef](#)]
53. Chen, G.; Hana, G.; Yanga, X. On the intrinsic shape of oceanic eddies derived from satellite altimetry. *Ocean Remote Sens. Environ.* **2019**, *228*, 75–89. [[CrossRef](#)]

Disclaimer/Publisher’s Note: The statements, opinions and data contained in all publications are solely those of the individual author(s) and contributor(s) and not of MDPI and/or the editor(s). MDPI and/or the editor(s) disclaim responsibility for any injury to people or property resulting from any ideas, methods, instructions or products referred to in the content.